

Full Paper

Hydrochemical characteristics and controlling factors of geothermal fluids during wet period in south-eastern Gansu seismic belt, China

Hanheng He¹, Lei Gao^{1,*}, Rengui Yang¹, Chun Liu¹ and Xianglong Yin²

¹ College of Geology and Jewelry, Lanzhou Vocational and Technical University of Resources and Environment, Lanzhou 730021, China

² The Third Geological Brigade of Jiangxi Provincial Geological Bureau, Jiujiang 332199, China

* Corresponding author, e-mail: leigao210278@lzre.edu.cn

Received: 2 August 2025 / Accepted: 27 April 2026 / Published: 29 April 2026

Abstract: Based on hydrogen and oxygen isotopes and hydrochemical composition data, this paper discusses the sources, genesis and geochemical changes of geothermal fluids in the south-eastern Gansu province. Water from six hot springs (Tongwei bathing pool River Hot Spring, Qingshui seismostation, Tianshui seismostation, Wushan seismostation, Chengxian seismostation and Wudu seismostation) was collected in triplicate from July to September in the wet season. The measurement results showed that total dissolved solids of the water samples ranged from 456-2823 mg/L. The water samples can be classified into four hydrochemical types: $\text{Na}^+\text{-Cl}^-$, $\text{Ca}^{2+}/\text{Na}^+\text{-HCO}_3^-$, $\text{Ca}^{2+}\text{-SO}_4^{2-}$ and $\text{Na}^+\text{-HCO}_3^-$. The hydrogen and oxygen isotopic composition indicates that the hot spring water in the region originates from atmospheric precipitation, undergoes water-rock interactions during its circulation, and may mix with surface water. The chemical composition of the water across different water bodies is primarily influenced by water-rock interactions and evaporation-crystallisation processes. Using the Gaillardet model, it is concluded that most ions result from the combined weathering and dissolution of silicate and evaporite rocks. The depth of hot water circulation exceeds 3 km, and significant changes in circulation depth have occurred since the Wenchuan earthquake.

Keywords: hot springs, south-eastern Gansu seismic belt, China, seismic zone, hydrochemical type

INTRODUCTION

The south-eastern region of Gansu lies on the northern edge of the West Qinling orogenic belt, at the intersection of north China, south China and Qinghai-Tibet blocks. The south-eastern region of Gansu is rich in geothermal resources and has developed multiple hot springs. At the same time, the region is structurally active and prone to frequent earthquakes, with a total of 44 earthquakes above M6 occurring since 183 BC [1-5]. Therefore, studying the tectonic activity in this region is especially important. Previous research has examined the hydrochemical characteristics and hot water circulation depth of several hot springs in the Longnan area of Tianshui and found that the flow rate, water temperature, radon in water, radon in gas, rare gases, and some ion concentrations of the hot springs have abnormal responses to seismic activity. For example, the water level and temperature of hot springs in Wudu, Tianshui and Qingshui showed abnormal fluctuations before and after the Wenchuan earthquake [6]. However, the understanding of the hydrochemical types and hot water sources of hot springs in south-eastern Gansu is still incomplete and the relationship between hydrochemical anomalies and seismic activity still lacks in-depth research. To investigate the tectonic activity in the border regions of Shaanxi, Gansu and Sichuan, water samples were collected from six hot springs in Tianshui, Longnan and surrounding areas. The study involved analysing the hydrochemical composition and hydrogen-oxygen isotopic characteristics of these hot springs and classifying their hydrochemical types. Additionally, the source and circulation depth of the hot water were examined. This study is significant for two reasons: first, it represents the initial effort to reveal the hydrochemical characteristics of geothermal springs in earthquake-prone areas; second, it enhances our understanding of contemporary hydrochemical processes in hot springs, contributing valuable insights for the geological environmental protection.

MATERIALS AND METHODS

Research Area

The south-eastern region of Gansu province is located at the intersection of the central east-west orogenic belt and the north-south seismic tectonic belt in China. It borders the Qilian orogenic belt to the north and the Bayan Har Songpan orogenic belt to the south. The overall location is sandwiched between two regional major faults, the East Kunlun Fault (F1) and the North Qinling Fault (F2) (Figure 1) and its geographical position is extremely important [7, 8]. The regional tectonic system is characterised by a series of nearly east-west thrust and strike slip faults distributed in a tile-like pattern between the two boundary faults, followed by a series of north-eastern trending Mesozoic and Cenozoic fault basins spanning the main structure.

Research Methods

After the arrival of the flood season, water samples were collected from 6 hot springs in Tongwei (GN1), Qingshui (GN2), Tianshui (GN3), Wushan (GN4), Chengxian (GN5) and Wudu (GN6) in mid-July, August and September 2021. The samples were collected in clean 1 L polyethylene bottles with a 0.45- μm filter membrane and the main testing parameters were Ca^{2+} , Mg^{2+} , Na^+ , K^+ , SO_4^{2-} , HCO_3^- , Cl^- , pH and total dissolved solids (TDS). Ca^{2+} , Mg^{2+} , Na^+ and K^+ were determined using flame atomic absorption spectroscopy; HCO_3^- was measured via hydrochloric acid titration; NO_3^- , SO_4^{2-} and Cl^- were analysed using ion chromatography; and TDS, temperature and pH were measured on-site with a multi-parameter water quality analyser. Isotopes

δD and $\delta^{18}O$ were determined using the isotope equilibrium method and a Finnigan MAT 253 mass spectrometer (precision: $\delta D \pm 2\text{‰}$, $\delta^{18}O \pm 0.2\text{‰}$) via the CO_2 - H_2O equilibrium method [9].

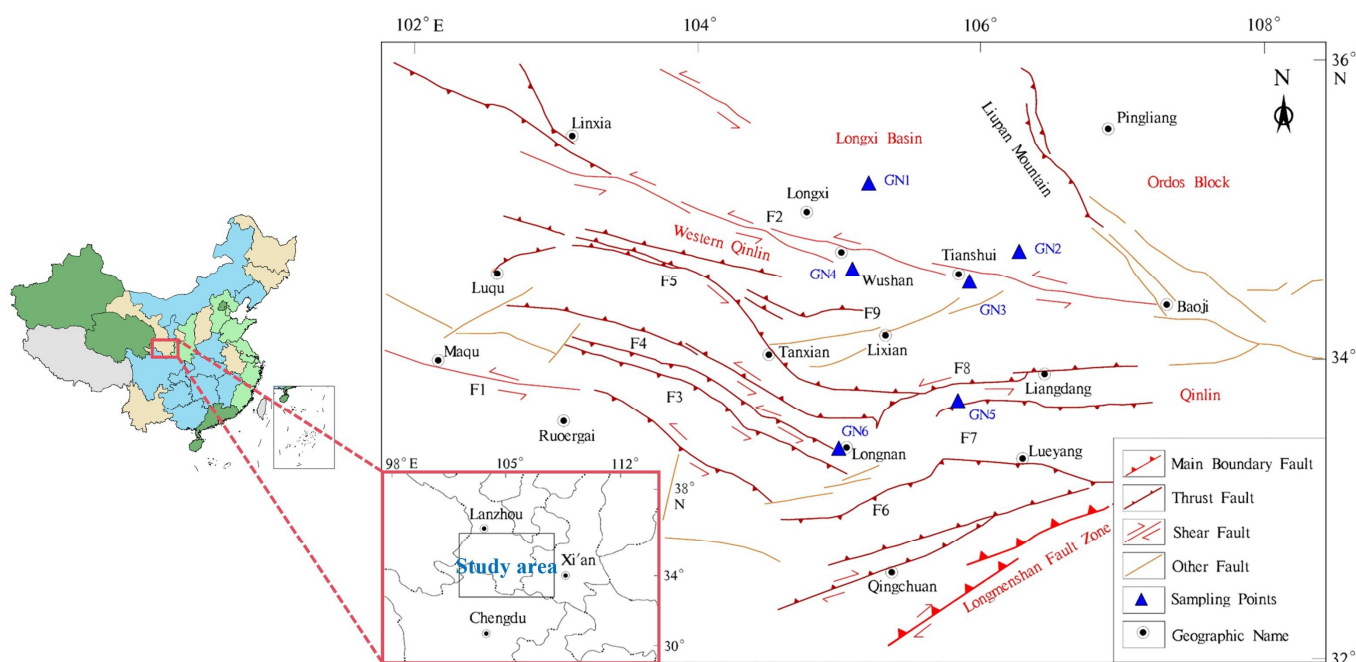


Figure 1. Geotectonic map and sampling distribution

Hydrochemical data were statistically analysed using Excel, in conjunction with the hydrogeological conditions of the study area [3]. Mathematical statistics, Pearson correlation analysis, Piper trilinear diagram, Gibbs diagram and ion ratio end-member diagrams were applied to comprehensively analyse hydrochemical characteristics and their controlling factors. Piper trilinear diagrams, Gibbs diagrams and ternary phase diagrams were plotted using Origin 2023 software (OriginLab, USA) while SPSS 26 (IBM, USA) was used for ion correlation analysis and systematic clustering analysis of hydrochemical characteristics.

RESULTS AND DISCUSSION

Hydrochemical Characteristics

Hydrochemical components

The measurement results are presented in Table 1. The average pH values of all hot spring water samples range from 6.9 to 8.6. Among the six water samples, three are medium-temperature hot water, accounting for 50% while the remaining samples have temperatures between 13°C and 23°C. Overall, water samples from the northern part of the study area exhibit higher temperatures, whereas those from the southern part are lower. The variation in mineralisation degree is significant, with an average range of 456–2823 mg/L. The mineralisation of hot spring water samples from Wushan (GN4) and Chengxian (GN5) is relatively low while the other samples show significantly higher mineralisation levels. Cations are mainly Na^+ and Ca^{2+} while the Ca^{2+} content in Wushan (GN4) hot spring is extremely low; anions such as SO_4^{2-} are highly present in most water samples, especially in Tianshui (GN3) hot springs, with a concentration of up to 1574.1 mg/L. However, in Wushan (GN4) hot springs, HCO_3^- dominates.

Table 1. Hydrochemical components

Sampling site	GN1	GN2	GN3	GN4	GN5	GN6
pH	7.735±0.10	7.560±0.12	6.932±0.11	8.537±0.09	7.435±0.04	7.105±0.08
T (°C)	50.2±1.29	51.1±1.31	13.0±0.33	23.0±0.59	34.0±0.87	18.0±0.46
TDS (mg/L)	1187±75.50	865±59.80	2823±218.52	456±18.01	616±22.00	1067±65.80
K ⁺ (mg/L)	9.7±1.23	10.1±0.72	7.3±0.53	2.5±0.42	0.9±0.66	7.5±1.31
Na ⁺ (mg/L)	391.1±26.82	294.9±3.26	240.1±13.87	115.0±9.69	9.4±0.59	119.8±11.68
Ca ²⁺ (mg/L)	138.9±6.69	95.3±2.49	295.6±3.20	5.7±0.49	45.7±4.02	110.6±6.92
Mg ²⁺ (mg/L)	3.0±0.42	1.7±0.49	153.5±7.72	2.9±0.42	14.4±0.24	132.7±6.60
SO ₄ ²⁻ (mg/L)	718.9±30.38	656.5±27.01	1623.4±79.18	54.7±5.87	80.2±4.22	757.8±32.47
HCO ₃ ⁻ (mg/L)	33.6±1.17	55.2±0.60	88.0±2.01	159.6±5.82	92.3±2.23	105.0±2.90
Cl ⁻ (mg/L)	269.8±12.88	86.8±3.01	44.3±0.78	12.5±0.92	5.6±0.36	137.4±5.80
NO ₃ ⁻ (mg/L)	2.0±0.09	2.1±0.06	6.5±0.78	0.4±0.24	9.7±0.80	1.6±0.11

Cluster analysis

Cluster analysis is a multivariate statistical classification method that groups and categorises different objects based on their similarities [10]. In this study it can be divided into sampling point clustering and hydrochemical index clustering. A comprehensive heat map clustering approach was used to analyse water samples from the study area. Figure 2 shows that the overall hydrochemical indicators can be grouped into two categories: the first category consists of TDS and SO₄²⁻ while the second category consists of pH, Ca²⁺, T, Mg²⁺, Na⁺, K⁺, Cl⁻, HCO₃⁻ and NO₃⁻. The sampling points are classified into three groups: GN3; GN4 and GN5; and GN1, GN2 and GN6. Based on the spatial distribution of sampling points and corresponding ion concentration analysis, GN3, characterised by the highest mineralisation and ion concentration, is classified as the first group and considered unstable. GN4 and GN5, with the lowest ion concentrations, are classified as the second group. GN1, GN2 and GN6, with stable and moderate ion concentrations, are classified as the third group.

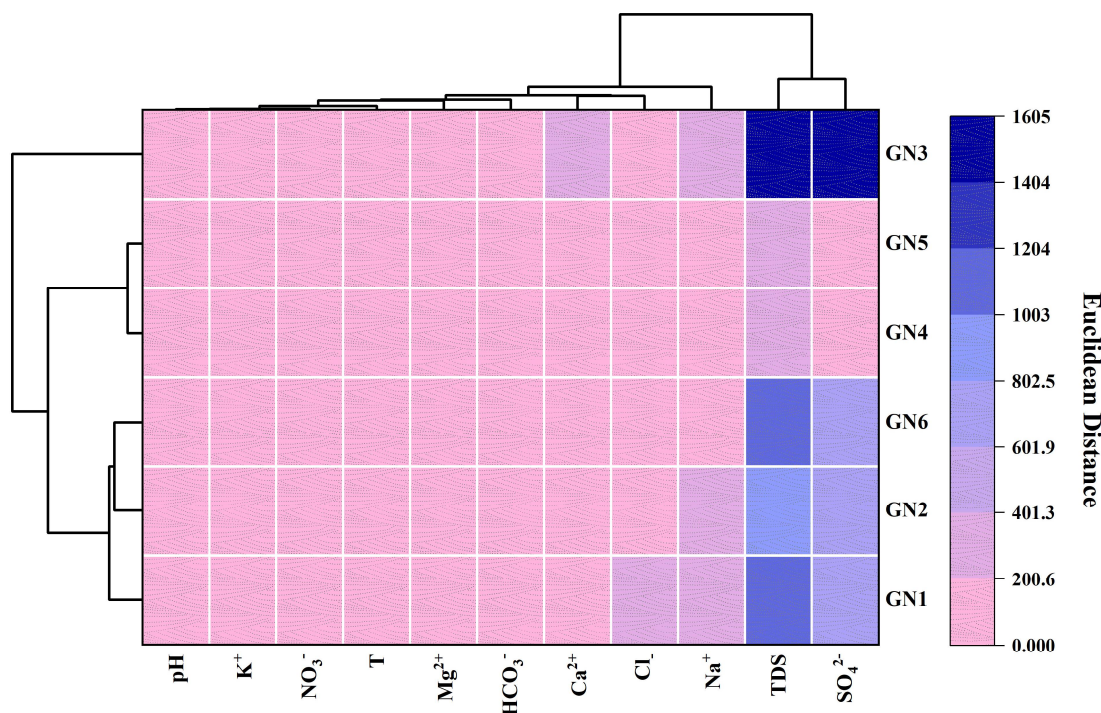


Figure 2. Cluster analysis heat map

Hydrochemical types

The hydrochemical types of hot springs are closely related to local geological structure, surrounding rock composition, hydrodynamics and geothermal conditions, reflecting lithological characteristics and water-rock interactions [11]. As shown in Figure 3, Tongwei (GN1) and Qingshui (GN2) hot springs are of the Na-Cl type. Their aquifers are composed of Lower-Middle Proterozoic metamorphic rocks, Yanshanian granite/granodiorite, and Tertiary clastic rocks and limestone. Soluble Na⁺ readily accumulates in groundwater while Cl⁻ enrichment may result from salt or marine sediment dissolution. Tianshui (GN3) and Wudu (GN6) hot springs belong to the SO₄²⁻-Ca²⁺ type, hosted in Upper Paleozoic marine-continental clastic rocks, limestone, mudstone and Cretaceous acidic intrusive rocks. Shallow groundwater circulation leads to low water temperatures. Cations (Na⁺, Mg²⁺) are derived from dolomite, calcite and gypsum dissolution. Abundant SO₄²⁻ and low HCO₃⁻ are likely due to sulfide oxidation generating sulfuric acid [12], followed by silicate hydrolysis and HCO₃⁻ consumption via carbonate reactions, resulting in near-neutral pH. Wushan (GN4) hot springs are of the HCO₃⁻-Na⁺ type, occurring in Indosinian porphyritic granite and Tertiary fluvio-lacustrine clastic rocks interbedded with gypsum. Na⁺ is the dominant cation while HCO₃⁻ dominates anions, forming weakly alkaline, low-mineralisation water. Na⁺ enrichment occurs during groundwater circulation and high HCO₃⁻ levels are attributed to CO₂ reactions with dissolved carbonates. Shallow water mixing further reduces mineralisation. Chengxian (GN5) hot springs are of the HCO₃⁻-Ca²⁺/Na⁺ type, hosted in Jurassic shallow marine clastic rocks, limestone, sandstone and Tertiary purple-red clay and gravel. Low Na⁺ and Cl⁻ concentrations are observed, with cations originating from carbonate/clastic rock weathering. HCO₃⁻ comes from carbonate/metamorphic rock dissolution while SO₄²⁻ is derived from sulfate rock dissolution or sulfide oxidation. Precipitation of these ions maintains low total dissolved solids.

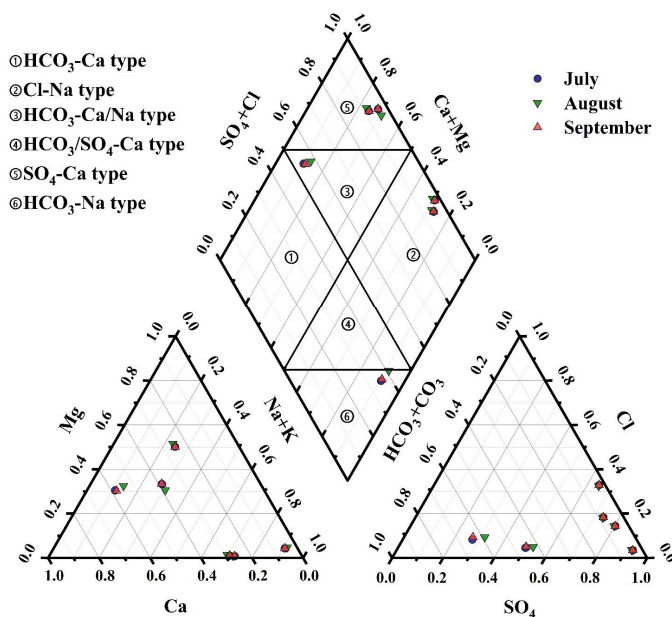


Figure 3. Piper three-line diagram of hydrochemical characteristics

Pearson correlation

The different ion indicators in surface water are interrelated rather than existing in isolation. A preliminary analysis of ion sources was conducted using Pearson correlation analysis. Figure 4 and Table 2 illustrates the varying degrees of correlation among the parameters of each indicator. The strength of these correlations can be further assessed using the critical correlation coefficient, as presented in Table 2. The correlation coefficients between TDS and Ca^{2+} and SO_4^{2-} are all greater than 0.8 while those with Mg^{2+} , Na^+ and K^+ exceed 0.6, indicating a strong correlation. This suggests that these ions are significant contributors to TDS. Additionally, the correlation coefficients among Ca^{2+} , Mg^{2+} and SO_4^{2-} are all greater than 0.6, with a particularly high correlation of 0.98 between SO_4^{2-} and Ca^{2+} , indicating they likely originate from the same source such as gypsum. Furthermore, the correlation coefficients among Na^+ , K^+ and Cl^- are also above 0.6, with Na^+ and K^+ showing a strong correlation of 0.85, suggesting these ions are likely derived from a common source such as potassium salt.

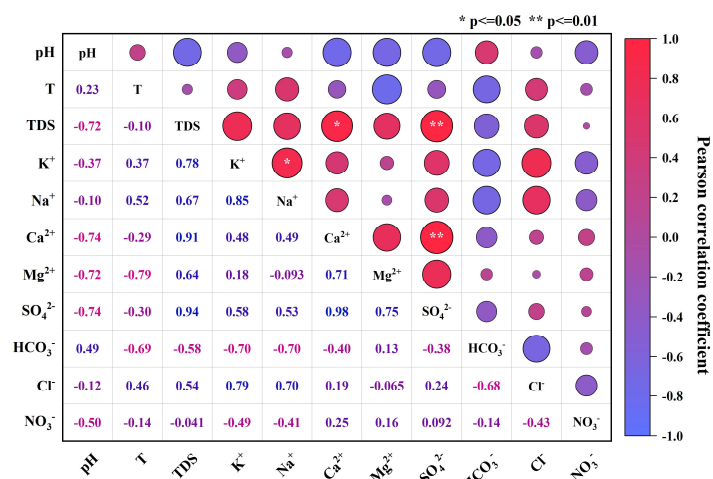


Figure 4. Pearson correlation coefficient plot of hydrochemical indices

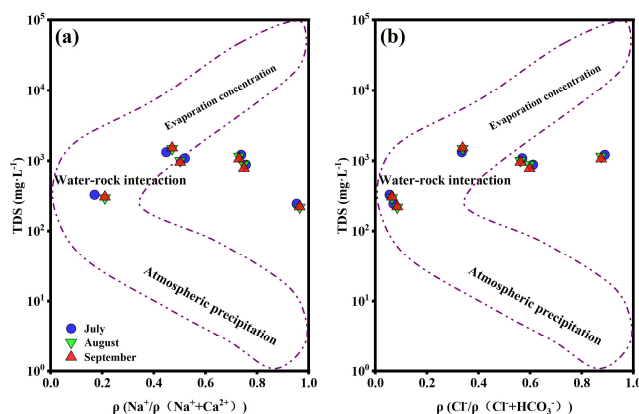
Table 2. Critical values of Pearson correlation coefficient

Pearson correlation coefficient	Correlation
0.8—1.0	Very strongly correlated
0.6—0.8	Strong correlation
0.4—0.6	Moderately related
0.2—0.4	Weak correlation
0.0—0.2	No relevance
<0.0	Negative correlation

Controlling Factors

Rock weathering

Throughout the year, HCO_3^- in surface water interacts with minerals in the riverbed while also being influenced by rainfall and evaporation. The Gibbs diagram visually illustrates the chemical composition characteristics, controlling factors and interrelationships of surface water samples, using a semi-logarithmic coordinate system [13]. This diagram is employed to analyse surface water samples collected from hot springs as shown in Figure 5.

**Figure 5.** Gibbs plot of hot springs

In the study area TDS of surface water samples range from 456 to 2823 $\text{mg}\cdot\text{L}^{-1}$ with the ratio of $\rho(\text{Na}^+)/\rho(\text{Na}^++\text{Ca}^{2+})$ varying between 0.1 and 1.0. Additionally, the ratio of $\rho(\text{Cl}^-)/\rho(\text{Cl}^-+\text{HCO}_3^-)$ is consistently less than 1, indicating significant variations influenced by geological structures and spring exposure conditions. GN5 is situated in a rock weathering control zone while GN3 and GN6 are influenced by evaporation crystallisation. GN2 and GN4 experience a combination of effects from rock weathering, evaporation concentration and atmospheric precipitation. These findings suggest that the primary mechanisms driving surface water formation in the study area are rock weathering and evaporation crystallisation, with atmospheric precipitation playing a relatively minor role.

Filtration effect

Analysing the proportional relationships between Mg^{2+} , Ca^{2+} and Na^+ ions provides insights into the formation of surface water [14, 15]. Figure 6 shows that the ratio of $\rho(Mg^{2+})/\rho(Na^+)$ ranges from 0.01 to 10 while that of $\rho(Mg^{2+})/\rho(Ca^{2+})$ exceeds 80% and remains below 1. These ratios suggest that the leaching processes of geothermal hot springs GN3, GN5 and GN6 are primarily driven by water-rock interactions. In contrast, evaporation plays a significant role in the formation of surface water in GN1, GN2 and GN4.

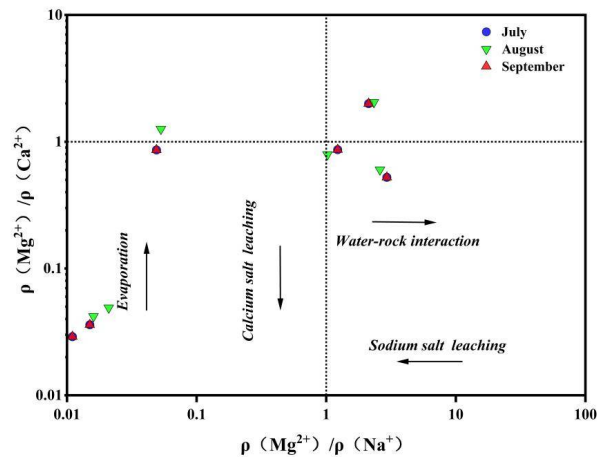


Figure 6. Distribution of ions in dissolution and filtration process of hot springs

Ion exchange

Under normal circumstances, cation exchange can lead to alterations in the concentrations of key ions in surface water, playing a significant role in shaping its chemical composition [16]. The ratio of $\rho(K^+ + Na^+ + Cl^-)/\rho(Ca^{2+} + Mg^{2+})$ helps determine whether cation exchange has occurred in surface water. A strong ion exchange would result in a fitted slope of approximately -1. However, as illustrated in Figure 7, the slope of the correlation among surface water samples ranges from -2.5 to -1.9, suggesting that only weak ion exchange may have taken place in this context. The chlor-alkali indices CAI_1 and CAI_2 are used to indicate cation exchange and its intensity [17]. When Na^+ and K^+ in water replace adsorbed Ca^{2+} and Mg^{2+} in riverbed minerals, CAI_1 and CAI_2 yield positive values. Conversely, when Ca^{2+} and Mg^{2+} in river water displace adsorbed Na^+ and K^+ in riverbed minerals, the indices produce negative values. The stronger the cation exchange interaction is the greater the absolute values of CAI_1 and CAI_2 become. The formulas for calculating CAI_1 and CAI_2 are as shown in equations (1) and (2) respectively. As shown in Figure 8, both CAI_1 and CAI_2 are negative and exhibit small absolute values, indicating a weak exchange of Ca^{2+} and Mg^{2+} for adsorbed Na^+ and K^+ in the riverbed minerals of the study area.

$$CAI_1 = \frac{Cl^- - (Na^+ + K^+)}{Cl^-} \quad (1)$$

$$CAI_2 = \frac{Cl^- - (Na^+ + K^+)}{HCO_3^- + SO_4^{2-} + CO_3^{2-} + HNO_3^-} \quad (2)$$

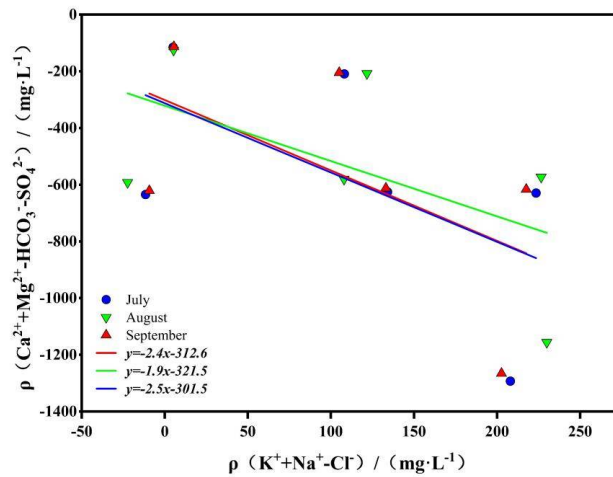


Figure 7. Relationship between $(K^++Na^++Cl^-)$ and $(Ca^{2+}+Mg^{2+}-HCO_3^- -SO_4^{2-})$ of hot springs

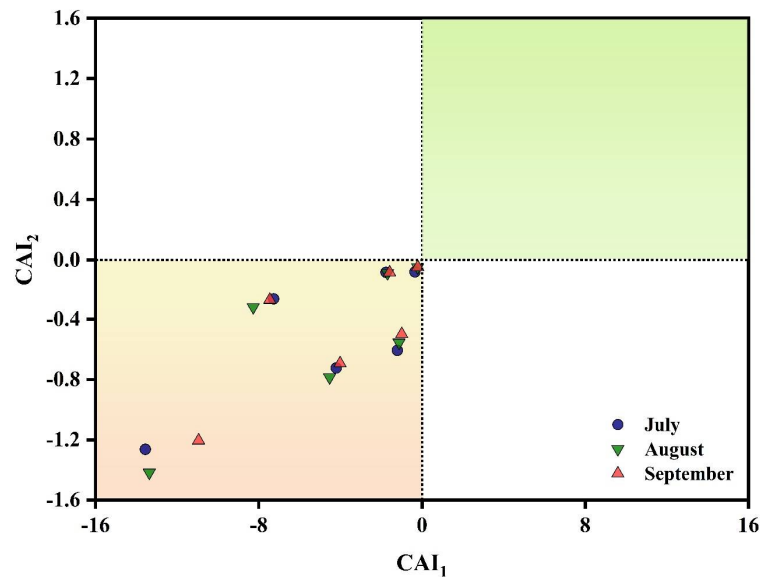


Figure 8. Relationship between CAI_1 and CAI_2 of hot springs

Main ion sources

This article employs the Gaillardet model to identify the type of rock weathering source influencing the hydrochemical composition of water bodies [18]. Analysing the relationships between Ca^{2+}/Na^+ and HCO_3^- /Na^+ , as well as Mg^{2+}/Na^+ concentrations from evaporite rocks, silicates and carbonates in the study area, reveals that surface water samples are predominantly associated with silicate and evaporite rocks. This suggests that the hot springs are significantly influenced by both the weathering and dissolution of silicate rocks, as well as by surface evaporation (Figure 9).

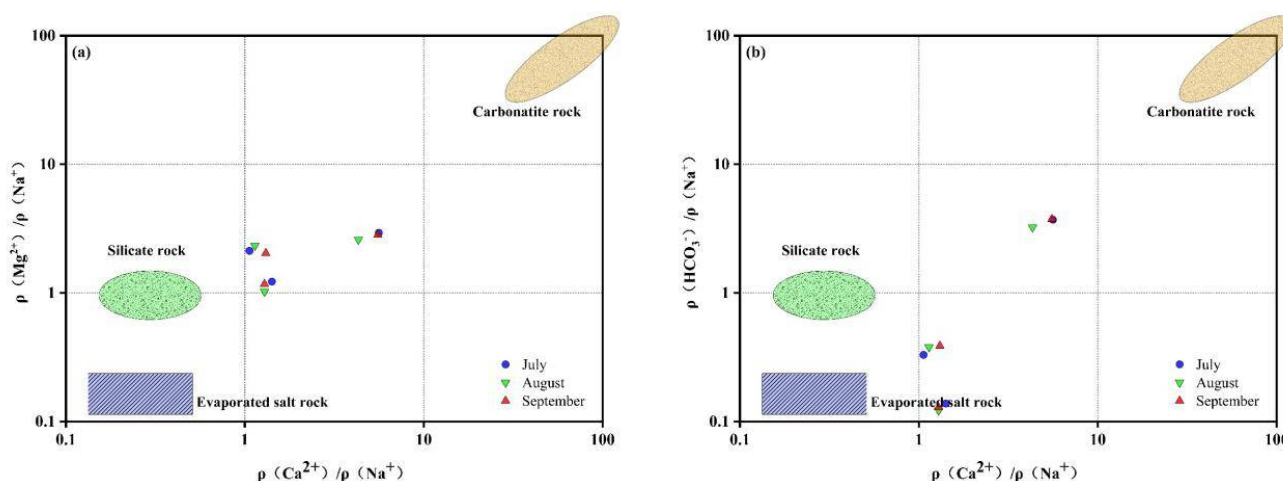


Figure 9. Concentration ratio relationship between $\text{Ca}^{2+}/\text{Na}^+$, $\text{Mg}^{2+}/\text{Na}^+$ and $\text{HCO}_3^-/\text{Na}^+$ of hot springs

Hydrogen and oxygen isotopes

Underground hot water sources can originate from magmatic water, metamorphic water or atmospheric precipitation. A linear relationship exists between δD and $\delta^{18}\text{O}$ in atmospheric precipitation. This study utilises the Global Meteoric Water Line; $\delta\text{D} = 8\delta^{18}\text{O} + 10$ [19] and Local Meteoric Water Line specific to northwest China; $\delta\text{D} = 7.38\delta^{18}\text{O} + 7.16$ [20-23]. Generally, the isotopic composition of hydrogen and oxygen in magmatic water falls within the ranges of $\delta^{18}\text{O} = 6\text{‰}$ to 10‰ and $\delta\text{D} = -80\text{‰}$ to -50‰ . For metamorphic water, the ranges are $\delta^{18}\text{O} = 5\text{‰}$ to 25‰ and $\delta\text{D} = -70\text{‰}$ to -20‰ . Figure 10 shows that the hydrogen and oxygen isotope compositions of hot spring water in the study area do not fall within these ranges, indicating that their source is atmospheric precipitation. Furthermore, the δD and $\delta^{18}\text{O}$ values of the hot spring water show significant deviations from atmospheric precipitation line. All six hot spring water samples are notably enriched in $\delta^{18}\text{O}$ and depleted in δD compared with atmospheric precipitation. This disparity arises because water undergoes isotope exchange reactions with surrounding rocks during circulation. After atmospheric precipitation infiltrates the ground, it engages in water-rock interactions, leading to a relative enrichment of $\delta^{18}\text{O}$ in the hot spring waters while δD remains largely unchanged. Consequently, the hot spring waters in the research area are derived from atmospheric precipitation and have experienced a certain degree of water-rock interaction. In particular, Wushan (GN4) is influenced by geological structures, rock lithology and hydrothermal conditions, resulting in a higher outlet temperature and relatively elevated $\delta^{18}\text{O}$ values.

Thermal storage temperature and depth

Before calculating the temperature of thermal storage and the depth of hot water circulation, it is necessary to determine whether the water-rock reaction has reached equilibrium. Generally, the Na-K-Mg triangle diagram is used to determine the water-rock equilibrium state. As shown in Figure 11, the water body can be divided into unbalanced water, partially balanced water and completely balanced water according to the degree of water-rock reaction. The analysis results show that except for the water samples from Tongwei (GN1), Qingshui (GN2) and Wushan (GN4), which are completely or partially balanced. The rest are unbalanced water, making it impossible to accurately estimate the temperature of the thermal storage. This article uses the cation-temperature scale method to estimate the temperature of the thermal storage. Cation-temperature scales include

K-Mg [24], Na-Li [25], Na-K [26] and Na-K-Ca [1] temperature scales.

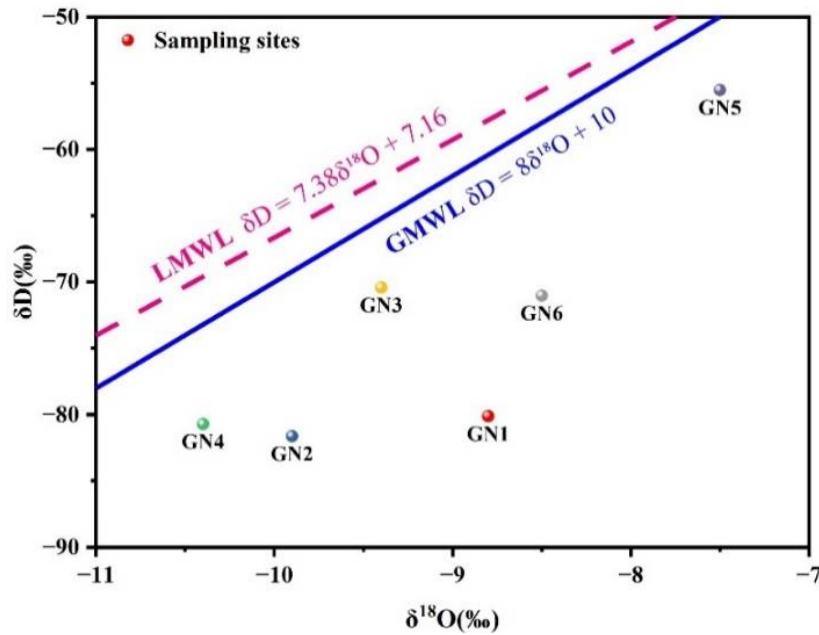


Figure 10. Hydrogen and oxygen isotopic composition of hot springs (LMWL = Local Meteoric Water Line, GMWL = Global Meteoric Water Line)

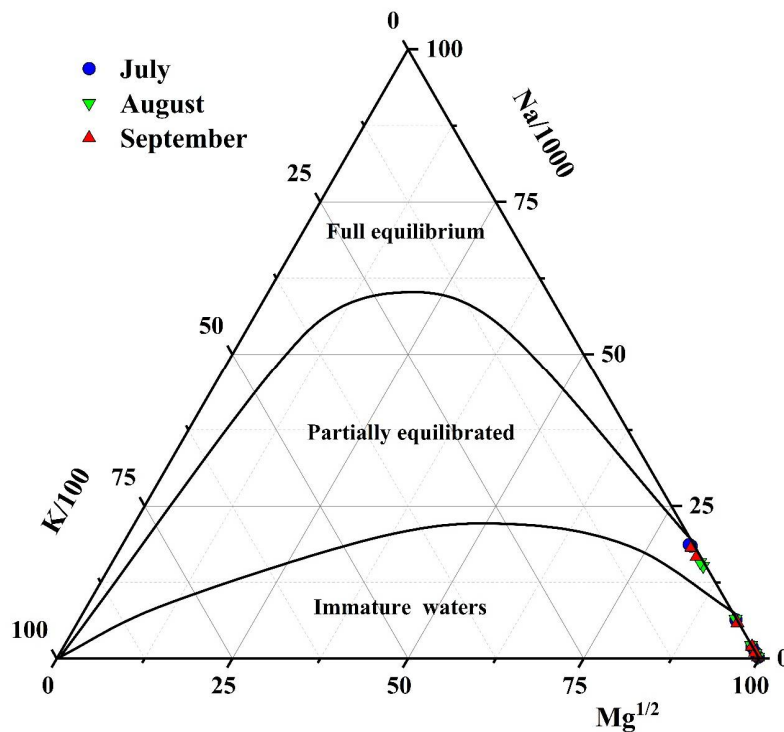


Figure 11. Na-K-Mg triangle diagram of hot springs

The formula for calculating the depth of underground hot water circulation is $Z = Z_0 + (T - T_0) / T_{grad}$, where Z is the depth of circulation (km); Z_0 is the depth of the isothermal

layer (km), with a value of 0.02 km; T is the thermal storage temperature ($^{\circ}\text{C}$); T₀ is the depth of the constant temperature layer ($^{\circ}\text{C}$), taking the local average temperature as 9.8°C ; T_{grad} is the ground temperature gradient ($^{\circ}\text{C}/\text{km}$), which refers to the change in ground temperature for every 1 km increase below the constant temperature layer. The average value of $30\text{-}40^{\circ}\text{C}/\text{km}$ is taken from south-eastern Gansu and the calculation results are shown in Table 3.

Table 3. Heat storage temperature and cycle depth

Sampling site	T _{Na-K} ($^{\circ}\text{C}$)	T _{K-Mg} ($^{\circ}\text{C}$)	T _{Na-Li} ($^{\circ}\text{C}$)	Average temperature ($^{\circ}\text{C}$)	Z(m)
GN1	124	113	145	127.3	3.37
GN2	137	122	148	135.7	3.61
GN4	133	146	249	176.0	4.76

The results indicate that the depth of hot water circulation in Tongwei (GN1), Qingshui (GN2) and Wushan (GN4) exceeds 3 km. This suggests that the faults in the study area are deep-seated shell faults and implies that the hot spring water circulation is substantial, leading to significant water-rock interactions. While the thermal storage temperature shows a linear correlation with the depth of hot spring water circulation, the degree of mineralisation does not positively correlate with circulation depth. This observation suggests that the surrounding rock type has a more pronounced impact on the extent of water-rock reactions. The unbalanced water observed in the hot springs of Tianshui (GN3), Chengxian (GN5) and Wudu (GN6) may result from the presence of smaller faults, shallower circulation depths, or the influence of atmospheric precipitation. Previous studies [27, 28] reported that the depths of hot spring water circulation in Qingshui and Wushan in 2006 were 5.16 km and 3.71 km respectively. In this study we found that following the Wenchuan earthquake in 2008, the depth of hot spring water circulation in Qingshui decreased by 1.55 km while in Wushan it increased by 1.05 km. This reinforces previous conclusions regarding the impact of seismic activity on the hydration characteristics of hot springs, specifically indicating that such activity alters groundwater transport conditions. This alteration is evidenced by the reduction in circulation depth in Qingshui and the increase in Wushan.

CONCLUSIONS

This article investigates the fluid geochemical and isotopic characteristics of six hot springs in the south-eastern Gansu province, focusing on how changes in hot spring hydration may reflect the impact of the 2008 Wenchuan surface-wave magnitude 8.0 earthquake. The following conclusions are drawn:

(1) The hot springs in the study area are generally neutral to weakly alkaline, with varying levels of TDS which are significantly higher in Tongwei, Tianshui, Qingshui and Wudu compared to Wushan and Chengxian due to differences in the surrounding rock types, water-rock interactions and surface water mixing. The hydrochemical composition is mainly shaped by water-rock interactions and evaporation crystallisation, with most ions stemming from the weathering and dissolution of silicate and evaporite rocks.

(2) Based on the chemical composition, the hot springs can be classified into four hydrochemical types: $\text{Na}^+\text{-Cl}^-$, $\text{Ca}^{2+}/\text{Na}^+\text{-HCO}_3^-$, $\text{Ca}^{2+}\text{-SO}_4^{2-}$ and $\text{Na}^+\text{-HCO}_3^-$. The primary ions are

Na⁺ and SO₄²⁻ and there are observable co-seismic and post-earthquake anomalies in hydration changes, with notable variations in K⁺, Ca²⁺, SO₄²⁻, Cl⁻, Na⁺ and HCO₃⁻ concentrations. In general K⁺ and Ca²⁺ levels increase while SO₄²⁻ and Cl⁻ concentrations decrease.

(3) The hot spring water sources are derived from atmospheric precipitation, with deep circulation and significant water-rock exchange reactions. The δ¹⁸O and δD values support this and the cluster analysis of hydrochemical indicators classifies the sampling points into three distinct groups. Major contributors to TDS are Ca²⁺, HCO₃⁻, Mg²⁺, Cl⁻ and SO₄²⁻, with HCO₃⁻ and Ca²⁺ from carbonates and SO₄²⁻ from a different source from gypsum.

ACKNOWLEDGEMENTS

This work was supported by Gansu Provincial Department of Education in the form of Industry Support Project (2023CYZC-76) and Gansu Province Education Science "14th Five-Year Plan" Project (GS[2024]GHBZX0035).

REFERENCES

1. R. O. Fournier and A. H. Truesdell, "An empirical Na/K/Ca geothermometer for natural waters", *Geochim. Cosmochim. Acta*, **1973**, 37, 1255-1275.
2. N. Robinson, J. Regetz and R. P. Guralnick, "EarthEnv-DEM90: A nearly-global, void-free, multi-scale smoothed, 90m digital elevation model from fused ASTER and SRTM data", *ISPRS J. Photogramm. Remote Sens.*, **2014**, 87, 57-67.
3. Z. Chen, X. Zhou, J. Du, C. Xie, L. Liu, Y. Li, L. Yi, H. Liu and Y. Cui, "Hydrochemical characteristics of hot spring waters in the Kangding District related to the Lushan MS7.0 earthquake in Sichuan, China", *Nat. Hazards Earth Syst. Sci.*, **2015**, 15, 1149-1156.
4. H. P. Ma, J. G. Feng, S. Y. Wu, R. Xu, Y. L. Huang, N. Li and Q. Wang, "The analysis of the abnormal characteristics of GPS data before the 2013 Minxian-Zhangxian MS 6.6 earthquake", *IOP Conf. Ser.: Earth Environ. Sci.*, **2018**, 153, Art.no.062044.
5. R. Xu and L. Wang, "Study on response spectra in the Loess region of Gansu, China", *Adv. Transdiscip. Eng.*, **2022**, 31, 788-795.
6. Wang. Z., "A preliminary report on the Great Wenchuan Earthquake", *Earthq. Eng. Eng. Vib.*, **2008**, 7, 225-234.
7. S. Li, Y. Wang, Z. Liang, S. He and W. Zeng, "Crustal structure in southeastern Gansu from regional seismic waveform inversion", *Chin. J. Geophys.*, **2012**, 55, 206-218.
8. W. Feng, Y. Tang and B. Hong, "Landslide hazard assessment methods along fault zones based on multiple working conditions: A case study of the Lixian-Luojiabu fault zone in Gansu Province (China)", *Sustainability*, **2022**, 14, Art.no.8098.
9. Yin. L, Hou. G, Su. X, Wang. D, Dong. J, Hao. Y and Wang. X, "Isotopes (δD and δ¹⁸O) in precipitation, groundwater and surface water in the Ordos Plateau, China: Implications with respect to groundwater recharge and circulation", *Hydrogeol. J.*, **2011**, 19, 429-443.
10. E. S. Dalmaijer, C. L. Nord and D. E. Astle, "Statistical power for cluster analysis", *BMC Bioinformatics*, **2022**, 23, Art.no.205.
11. M. Piper, "A graphic procedure in the geochemical interpretation of water-analyses", *Eos Trans. Amer. Geophys. Union*, **1944**, 25, 914-928.
12. Q. Guo, "Hydrogeochemistry of high-temperature geothermal systems in China: A review", *Appl. Geochem.*, **2012**, 27, 1887-1898.

13. R. J. Gibbs, "Mechanisms controlling world water chemistry", *Science*, **1970**, *170*, 1088-1090.
14. J. Bian, W. Sun, J. Li, Y. Li, Y. Ma and Y. Li, "Hydrochemical formation mechanism of mineral springs in Changbai Mountain (China)", *Environ. Earth Sci.*, **2023**, *82*, Art.no.145.
15. M. Yan, L. Wang, Q. Wang and Z. Liu, "Hydrochemical characteristics and origin analysis of groundwater in Nanling County, Anhui Province", *Water*, **2024**, *16*, Art.no.1579.
16. S. Jiang, H. Sun, H. Wang, B. P. Ladewig and Z. Yao, "A comprehensive review on the synthesis and applications of ion exchange membranes", *Chemosphere*, **2021**, *282*, Art.no. 130817.
17. A. K. Tiwari and A. K. Singh, "Hydrogeochemical investigation and groundwater quality assessment of Pratapgarh District, Uttar Pradesh", *J. Geol. Soc. India*, **2014**, *83*, 329-343.
18. J. Gaillardet, B. Dupré and C. J. Allègre, "A global geochemical mass budget applied to the Congo Basin rivers: Erosion rates and continental crust composition", *Geochim. Cosmochim. Acta*, **1995**, *59*, 3469-3485.
19. H. Craig, "The geochemistry of the stable carbon isotopes", *Geochim. Cosmochim. Acta*, **1953**, *3*, 53-92.
20. T. Rigaudier, V. Gardien, F. Martineau, G. Reverdy and C. Lécuyer, "Hydrogen and oxygen isotope reference materials for the analysis of water inclusions in halite", *Geostand. Geoanal. Res.*, **2012**, *36*, 51-59.
21. B. Chimeddorj, D. Munkhbat, B. Altanbaatar, O. Dolgorjav and B. Oyuntsetseg, "Hydrogeochemical characteristics and geothermometry of hot springs in the Altai Region, Mongolia", *Geochem.: Explor. Environ. Anal.*, **2021**, *21*, Art.no. geochem2021-016.
22. C. Li, X. Zhou, Y. Yan, S. Ouyang and F. Liu, "Hydrogeochemical characteristics of hot springs and their short-term seismic precursor anomalies along the Xiaojiang fault zone, Southeast Tibet Plateau", *Water*, **2021**, *13*, Art.no.2638.
23. R. Zhou, X. Zhou, Y. Li, M. He, J. Li, J. Dong, J. Tian, K. Li, Y. Yan, S. Ouyang, F. Liu and Z. Luo, "Hydrogeochemical and isotopic characteristics of the hot springs in the Litang Fault Zone, Southeast Qinghai-Tibet Plateau", *Water*, **2022**, *14*, Art.no.1496.
24. W. F. Giggenbach, "Geothermal solute equilibria. Derivation of Na-K-Mg-Ca ge indicators", *Geochim. Cosmochim. Acta*, **1988**, *52*, 2749-2765.
25. S. P. Verma and E. Santoyo, "New improved equations for NaK, NaLi and SiO₂ geothermometers by outlier detection and rejection", *J. Volcanol. Geotherm. Res.*, **1997**, *79*, 9-23.
26. I. Can, "A new improved Na/K geothermometer by artificial neural networks", *Geothermics*, **2002**, *31*, 751-760.
27. Liu-Zeng, Y. Klinger, X. Xu, C. Lasserre, G. Chen, W. Chen, P. Tapponnier and B. Zhang, "Millennial recurrence of large earthquakes on the Haiyuan fault near Songshan, Gansu Province, China", *Bull. Seismol. Soc. Amer.*, **2007**, *97*, 14-34.
28. F. B. Liu and A. G. Wang and W. Pang, "Research on static stress triggering and seismicity in Minxian and adjacent area, Gansu", *Appl. Mech. Mater.*, **2013**, *477-478*, 1075-1083.